Amino Acids (2015) 47:813–823
DOI 10.1007/s00726-014-1911-z

ORIGINAL ARTICLE

Tc-99m-labeled RGD-conjugated alpha-melanocyte stimulating hormone hybrid peptides with reduced renal uptake

Jianquan Yang · Chien-An A. Hu · Yubin Miao

Received: 28 October 2014 / Accepted: 24 December 2014 / Published online: 4 January 2015

Abstract The purpose of this study was to examine whether the replacement of the positively-charged Lys or Arg linker with a neutral linker could reduce the renal uptake of Arg-Gly-Asp (RGD)-conjugated alpha-melanocyte stimulating hormone (α-MSH) hybrid peptide. The RGD motif {cyclic(Arg-Gly-Asp-DTyr-Asp)} was coupled to [Cys^{3,4,10}, D-Phe^{7}, Arg^{11}]α-MSH$_{3-13}$ {(Arg^{11})CCMSH} through the neutral βAla or Ahx {aminohexanoic acid} linker (replacing the Lys or Arg linker) to generate novel RGD-βAla-(Arg^{11})CCMSH and RGD-Ahx-(Arg^{11})CCMSH hybrid peptides. The receptor-binding affinity and cytotoxicity of RGD-βAla-(Arg^{11})CCMSH and RGD-Ahx-(Arg^{11})CCMSH were determined in B16/F1 melanoma cells. The melanoma targeting and imaging properties of ^{99m}Tc-RGD-βAla-(Arg^{11})CCMSH and ^{99m}Tc-RGD-Ahx-(Arg^{11})CCMSH were determined in B16/F1 melanoma-bearing C57 mice. The replacement of the Lys or Arg linker with the βAla or Ahx linker retained nanomolar receptor-binding affinities and remarkable cytotoxicity of RGD-βAla-(Arg^{11})CCMSH and RGD-Ahx-(Arg^{11})CCMSH. The receptor-binding affinities of RGD-βAla-(Arg^{11})CCMSH and RGD-Ahx-(Arg^{11})CCMSH were 0.8 ± 0.05 and 1.3 ± 0.1 nM. Three-hour incubation with 0.1 μM of RGD-βAla-(Arg^{11})CCMSH and RGD-Ahx-(Arg^{11})CCMSH decreased the survival percentages of B16/F1 cells by 71 and 67 % as compared to the untreated control cells 5 days post the treatment. The replacement of the Arg linker with the βAla or Ahx linker reduced the non-specific renal uptake of ^{99m}Tc-RGD-βAla-(Arg^{11})CCMSH and ^{99m}Tc-RGD-Ahx-(Arg^{11})CCMSH by 62 and 61 % at 2 h post-injection. ^{99m}Tc-RGD-βAla-(Arg^{11})CCMSH displayed higher melanoma uptake than ^{99m}Tc-RGD-Ahx-(Arg^{11})CCMSH at 0.5, 2, 4, and 24 h post-injection. Enhanced tumor to kidney uptake ratio of ^{99m}Tc-RGD-βAla-(Arg^{11})CCMSH warranted the further evaluation of ^{188}Re-labeled RGD-βAla-(Arg^{11})CCMSH as a novel MC1 receptor-targeting therapeutic peptide for melanoma treatment in the future.

Keywords Arg-Gly-Asp · Alpha-melanocyte stimulating hormone hybrid peptide · Melanoma imaging

Handling Editor: F. Albericio.

J. Yang · Y. Miao
College of Pharmacy, University of New Mexico, Albuquerque, NM 87131, USA

C.-A. A. Hu
Department of Biochemistry and Molecular Biology, University of New Mexico, Albuquerque, NM 87131, USA

C.-A. A. Hu · Y. Miao
Cancer Research and Treatment Center, University of New Mexico, Albuquerque, NM 87131, USA

Y. Miao
Department of Dermatology, University of New Mexico, Albuquerque, NM 87131, USA

Y. Miao (✉)
College of Pharmacy, University of New Mexico, 2502 Marble NE, MSC09 5360, Albuquerque, NM 87131-0001, USA
e-mail: ymiao@salud.unm.edu

Introduction

G protein-coupled melanocortin-1 (MC1) receptors are over-expressed in human and murine melanoma cells (Chen et al. 2000; Guo et al. 2009a, b, c; Miao et al. 2003; Siegrist et al. 1989; Tatro et al. 1987; Yang et al. 2010a, b), making the MC1 receptor a distinct molecular target.

Targeting the MC1 receptors can differentiate melanoma cells from normal cells due to the higher levels of the MC1 receptors on melanoma cells. Thus, both linear and cyclic alpha-melanocyte-stimulating hormone (α-MSH) peptide radiopharmaceuticals have been reported to target the MC1 receptors for melanoma detection and treatment (Chen et al. 2001; Cheng et al. 2002, 2007; Froidevaux et al. 2002, 2004, 2005; Guo et al. 2009a, b, c, 2010; Miao et al. 2002, 2005a, b, 2007, 2008; Wei et al. 2007). Recently, we have reported a novel class of Arg-Gly-Asp-conjugated α-MSH hybrid peptides targeting the MC1 receptors for potential melanoma imaging and therapy (Yang et al. 2009, 2010a, b). The RGD motif {cyclic(Arg-Gly-Asp-DTyr-Asp)} was used as an apoptosis inducer and was conjugated to the [$Cys^{3,4,10}$, D-Phe^{7}, Arg^{11}]α-MSH_{3-13} {(Arg^{11})CCMSH} peptide through a Lys linker to yield RGD-Lys-(Arg^{11})CCMSH hybrid peptide (Yang et al. 2009). RGD-Lys-(Arg^{11})CCMSH showed remarkable clonogenic cytotoxic effect in B16/F1 melanoma cells. Three-hour incubation with 0.1 μM of RGD-Lys-(Arg^{11})CCMSH decreased 65 % of the clonogenic survival of B16/F1 cells as compared to the untreated control cells six days post treatment. Meanwhile, ^{99m}Tc-RGD-Lys-(Arg^{11})CCMSH displayed high B16/F1 melanoma uptake of 14.83 ± 2.94 % ID/g at 2 h post-injection (Yang et al. 2009). However, relatively high non-specific renal uptake of ^{99m}Tc-RGD-Lys-(Arg^{11})CCMSH (67.12 ± 8.79 % ID/g at 2 h post-injection) needed to be reduced to facilitate further evaluation of the α-MSH hybrid peptide for melanoma therapy in melanoma-bearing mice (Yang et al. 2009).

Recently, we found that the substitution of the Lys linker with the Arg linker dramatically improved the melanoma uptake by 44 % and reduced the renal uptake by 36 % at 2 h post-injection (Yang et al. 2010b). RGD-Arg-(Arg^{11})CCMSH displayed similar remarkable clonogenic cytotoxic effect as RGD-Lys-(Arg^{11})CCMSH in B16/F1 melanoma cells (Yang et al. 2010b). Importantly, co-injection of 15 mg of L-lysine substantially decreased the renal uptake of ^{99m}Tc-RGD-Lys-(Arg^{11})CCMSH by 52 % and the renal uptake of ^{99m}Tc-RGD-Arg-(Arg^{11})CCMSH by 28 % at 2 h post-injection, indicating that the overall positive charges of ^{99m}Tc-RGD-Lys-(Arg^{11})CCMSH and ^{99m}Tc-RGD-Arg-(Arg^{11})CCMSH contributed to their non-specific renal uptake (Yang et al. 2010b). Therefore, we hypothesized that further reduction of the overall positive charge of the ^{99m}Tc-labeled RGD-conjugated α-MSH hybrid peptide would further decrease its non-specific renal uptake. To examine our hypothesis, we synthesized two novel RGD-conjugated α-MSH hybrid peptides with less positive charges in this study. The RGD motif was coupled to the (Arg^{11})CCMSH peptide through the neutral βAla or Ahx hydrocarbon linker to generate new RGD-βAla-(Arg^{11})CCMSH and RGD-Ahx-(Arg^{11})CCMSH hybrid peptides. The neutral βAla and Ahx hydrocarbon linkers were used to replace the positively-charged Lys or Arg linker to decrease the overall positive charges of RGD-βAla-(Arg^{11})CCMSH and RGD-Ahx-(Arg^{11})CCMSH. We determined the receptor-binding affinities and cytotoxicity of RGD-βAla-(Arg^{11})CCMSH and RGD-Ahx-(Arg^{11})CCMSH in B16/F1 melanoma cells. Meanwhile, we examined melanoma targeting and imaging properties of ^{99m}Tc-RGD-βAla-(Arg^{11})CCMSH and ^{99m}Tc-RGD-Ahx-(Arg^{11})CCMSH in B16/F1 melanoma-bearing mice.

Materials and methods

Chemicals and reagents

Amino acids and resin were purchased from Advanced ChemTech Inc. (Louisville, KY) and Novabiochem (San Diego, CA). ^{125}I-Tyr^{2}-[Nle^{4}, D-Phe^{7}]-α-MSH {^{125}I-(Tyr^{2})-NDP-MSH} was obtained from PerkinElmer, Inc. (Shelton, CT) for in vitro receptor-binding assay. $^{99m}TcO_4^-$ was purchased from Cardinal Health (Albuquerque, NM) for peptide radiolabeling. Cyclo(Arg-Gly-Asp-DPhe-Val) {RGD} peptide was purchased from Enzo Life Sciences (Plymouth Meeting, PA) for peptide blocking studies. All other chemicals used in this study were purchased from Thermo Fischer Scientific (Waltham, MA) and used without further purification. B16/F1 murine melanoma cells were obtained from American Type Culture Collection (Manassas, VA).

Peptide synthesis

New RGD-βAla-(Arg^{11})CCMSH and RGD-Ahx-(Arg^{11})CCMSH peptides were synthesized on Sieber amide resin using fluorenylmethyloxycarbonyl (Fmoc) chemistry by an Advanced ChemTech multiple-peptide synthesizer (Louisville, KY) according to our published procedure (Yang et al. 2009) with modifications. Briefly, 70 μmol of Sieber amide resin and 210 μmol of Fmoc-protected amino acids were used for the synthesis. Fmoc-βAla and Fmoc-Ahx were used to generate the βAla and Ahx linkers in the hybrid peptides, respectively. The intermediate scaffolds of H_2N-Arg(Pbf)-Ala-Asp(OtBu)-DTyr(tBu)-Asp(*O*-2-phenylisopropyl)-βAla/Ahx-Cys(Trt)-Cys(Trt)-Glu(OtBu)-His(Trt)-DPhe-Arg(Pbf)-Trp(Boc)-Cys(Trt)-Arg(Pbf)-Pro-Val were synthesized on H_2N-Sieber amide resin by an Advanced ChemTech multiple-peptide synthesizer (Louisville, KY). The protecting groups of 2-phenylisopropyl were removed and the peptides were cleaved from the resin treating with a mixture of 2.5 % of trifluoroacetic acid (TFA) and 5 % of triisopropylsilane. After the precipitation with ice-cold ether and characterization by liquid chromatography-mass spectroscopy (LC-MS), the protected peptides were dissolved in

H_2O/CH_3CN (50:50) and lyophilized to remove the reagents such as TFA and triisopropylsilane. The protected peptides were further cyclized by coupling the carboxylic group from the Asp with the alpha-amino group from the Arg at the N-terminus. The cyclization reaction was achieved by overnight reaction in dimethylformamide (DMF) using benzotriazole-1-*yl*-*oxy*-*tris*-pyrrolidino-phosphonium-hexafluorophosphate (PyBOP) as a coupling agent in the presence of *N,N*-diisopropylethylamine (DIEA). After characterization by LC–MS, the cyclized protected peptides were dissolved in H_2O/CH_3CN (50:50) and lyophilized to remove the reagents. The protecting groups were totally removed by treating with a mixture of trifluoroacetic acid (TFA), thioanisole, phenol, water, ethanedithiol, and triisopropylsilane (87.5:2.5:2.5:2.5:2.5:2.5) for 2 h at room temperature (25 °C). The peptides were precipitated and washed with ice-cold ether for four times, purified by reverse phase-high performance liquid chromatography (RP-HPLC) and characterized by LC–MS.

In vitro receptor-binding assay

The IC_{50} values of RGD-βAla-(Arg^{11})CCMSH and RGD-Ahx-(Arg^{11})CCMSH for MC1 receptor were determined in B16/F1 melanoma cells. The receptor-binding assay was replicated in triplicate for each peptide. Briefly, the B16/F1 cells in 24-well cell culture plates (5×10^5/well) were incubated at room temperature (25 °C) for 2 h with approximately 40,000 counts per minute (cpm) of ^{125}I-(Tyr^2)-NDP-MSH in the presence of increasing concentrations (10^{-12} to 10^{-5} M) of either RGD-βAla-(Arg^{11})CCMSH or RGD-Ahx-(Arg^{11})CCMSH in 0.3 mL of binding medium {Modified Eagle's medium with 25 mM *N*-(2-hydroxyethyl)-piperazine-*N*'-(2-ethanesulfonic acid), pH 7.4, 0.2 % bovine serum albumin (BSA), 0.3 mM 1,10-phenathroline}. The medium was aspirated after the incubation. The cells were rinsed twice with 0.5 mL of ice-cold pH 7.4, 0.2 % BSA/0.01 M phosphate buffered saline (PBS) and lysed in 0.5 mL of 1 N NaOH for 5 min. The activities associated with cells were measured in a Wallac 1480 automated gamma counter (PerkinElmer, Waltham, MA). The IC_{50} values were calculated using Prism software (GraphPad Software, La Jolla, CA).

Cytotoxicity of RGD-βAla-(Arg^{11})CCMSH and RGD-Ahx-(Arg^{11})CCMSH

The B16/F1 cells were seeded in 96-well plates (150 cells/well) and incubated in a CO_2 incubator overnight. After being washed once with the culture medium (RPMI 1640 medium), the cells were incubated at 37 °C for 3 h in the presence of 0.1 μM of RGD-βAla-(Arg^{11})CCMSH, RGD-Ahx-(Arg^{11})CCMSH, (Arg^{11})CCMSH or RGD in 0.1 mL of the binding medium, respectively. The control cells were only incubated in the culture medium. After the incubation, the binding medium was aspirated. The cells were washed with culture medium once and returned to the CO_2 incubator to form colonies over 5 days in the culture medium. The culture medium was changed every other day. After 5 days, the culture medium was aspirated and the cells were incubated with 0.1 mL of 3-(4,5-dimethylthiazole-2-yl)-2,5-diphenyl tetrazolium bromide (MTT) solution (0.5 mg/mL in PBS, pH 7.4) at 37 °C for 3 h until intracellular punctate purple precipitate (formazan) were observed. The formazan crystals yielded were dissolved in 0.1 mL of 0.1 N acidic anhydrous isopropanol. Spectrophotometric absorbance was measured at the wavelengths of 570 nm and 630 nm (as a control) using an microplate reader (SpectraMax 340, Molecule Devices), respectively. The absorbance of cells was calculated by substracting the value at 630 nm from the value at 570 nm. The percentage of survived cells was calculated as percentage survival = (absorbance of treated cells/absorbance of control cells) × 100 %.

Peptide radiolabelling

The RGD-βAla-(Arg^{11})CCMSH and RGD-Ahx-(Arg^{11})CCMSH peptides were radiolabeled with ^{99m}Tc via a glucoheptonate transchelation reaction according to our published procedure (Yang et al. 2009). Briefly, $^{99m}TcO_4^-$ (~74 MBq) was reduced by $SnCl_2$ to form ^{99m}Tc-glucoheptonate at 25 °C in the first step. Then 10 μg of RGD-βAla-(Arg^{11})CCMSH or RGD-Ahx-(Arg^{11})CCMSH was added into the reaction vial to compete off the glucoheptonate at 75 °C to yield ^{99m}Tc-RGD-βAla-(Arg^{11})CCMSH or ^{99m}Tc-RGD-Ahx-(Arg^{11})CCMSH. For stability, biodistribution and imaging studies, each radiolabeled peptide was purified to single species by Waters RP-HPLC (Milford, MA) on a Grace Vydac C-18 reverse-phase analytical column (Deerfield, IL) using a 20-min gradient of 18-28 % acetonitrile in 20 mM HCl aqueous solution at a 1 mL/min flow rate. The stability of ^{99m}Tc-RGD-βAla-(Arg^{11})CCMSH and ^{99m}Tc-RGD-Ahx-(Arg^{11})CCMSH was determined by incubation in mouse serum at 37 °C for 24 h and monitored for degradation by RP-HPLC.

Biodistribution and melanoma imaging studies

All the animal studies were conducted in compliance with Institutional Animal Care and Use Committee approval. The biodistribution properties of ^{99m}Tc-RGD-βAla-(Arg^{11})CCMSH and ^{99m}Tc-RGD-Ahx-(Arg^{11})CCMSH were determined in B16/F1 melanoma-bearing C57 female mice (Harlan, Indianapolis, IN). The C57 mice were subcutaneously inoculated in the right flank with 1×10^6 B16/F1 cells. The weight of tumors reached approximately 0.2 g

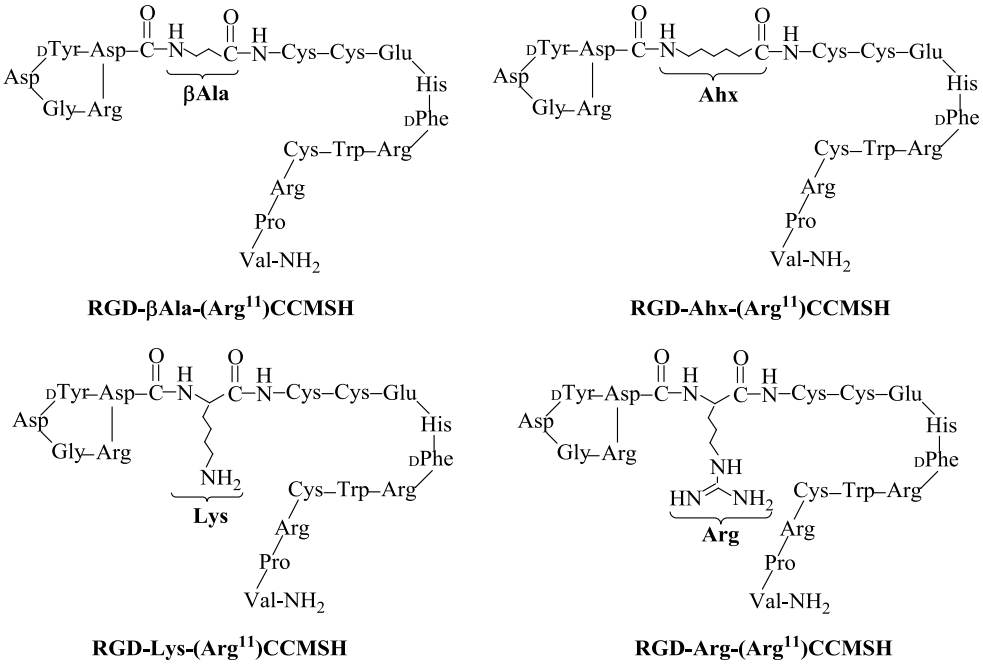

Fig. 1 Schematic structures of RGD-βAla-(Arg^{11})CCMSH, RGD-Ahx-(Arg^{11})CCMSH, RGD-Lys-(Arg^{11})CCMSH and RGD-Arg-(Arg^{11})CCMSH. The structures of RGD-Lys-(Arg^{11})CCMSH and RGD-Arg-(Arg^{11})CCMSH were cited from the references (Yang et al. 2009, 2010b) for comparison

10 days post cell inoculation. Each melanoma-bearing mouse was injected with 0.037 MBq of ^{99m}Tc-RGD-βAla-(Arg^{11})CCMSH or ^{99m}Tc-RGD-Ahx-(Arg^{11})CCMSH via the tail vein. Groups of 5 mice were sacrificed at 0.5, 2, 4, and 24 h post-injection, and tumors and organs of interest were harvested, weighed and counted in a gamma counter. Blood values were taken as 6.5 % of the whole-body weight. The specificity of the tumor uptake was determined by co-injecting ^{99m}Tc-RGD-βAla-(Arg^{11})CCMSH or ^{99m}Tc-RGD-Ahx-(Arg^{11})CCMSH with 10 μg (6.1 nmol) of unlabeled NDP-MSH or 3.5 μg (6.1 nmol) of RGD peptide at 2 h post-injection.

To determine the melanoma imaging properties, approximately 6.1 MBq of ^{99m}Tc-RGD-βAla-(Arg^{11})CCMSH or ^{99m}Tc-RGD-Ahx-(Arg^{11})CCMSH was injected into B16/F1 melanoma-bearing C57 mice via the tail vein, respectively. The mice were anesthetized with 1.5 % isoflurane for small animal SPECT/CT (Nano-SPECT/CT®, Bioscan, Washington DC) imaging 2 h post-injection. The 9-min CT imaging was immediately followed by the SPECT imaging of whole-body. The SPECT scans of 24 projections were acquired. Reconstructed data from SPECT and CT were visualized and co-registered using InVivoScope (Bioscan, Washington DC).

Effect of co-injection of L-lysine on renal uptake

In attempt to further understand the roles of βAla and Ahx linkers in the renal uptake, the effect of L-lysine co-injection on the renal uptake of ^{99m}Tc-RGD-βAla-(Arg^{11})CCMSH and ^{99m}Tc-RGD-Ahx-(Arg^{11})CCMSH was examined in B16/F1 melanoma-bearing C57 mice. Two groups of 5 mice were injected with an aqueous mixture of 0.037 MBq of ^{99m}Tc-RGD-βAla-(Arg^{11})CCMSH and 15 mg of L-lysine or an aqueous mixture of 0.037 MBq of ^{99m}Tc-RGD-Ahx-(Arg^{11})CCMSH and 15 mg of L-lysine, respectively. The mice were sacrificed at 2 h post-injection, and tumors and kidneys were harvested, weighed and counted in a gamma counter.

Statistical analysis

Statistical analysis was performed using the Student's *t* test for unpaired data to determine the significance of differences in tumor and kidney in biodistribution and co-injection of L-lysine studies, as well as the significance of differences in untreated control and treatment groups in cytotoxicity studies described above. Differences at the 95 % confidence level ($p < 0.05$) were considered significant.

Results

New RGD-βAla-(Arg^{11})CCMSH and RGD-Ahx-(Arg^{11})CCMSH were synthesized using Fmoc chemistry and purified by RP-HPLC. Figure 1 illustrates the structures of RGD-βAla-(Arg^{11})CCMSH and RGD-Ahx-(Arg^{11})CCMSH. The structures of RGD-Lys-(Arg^{11})CCMSH and RGD-Arg-(Arg^{11})CCMSH were cited for comparison. The peptide identities were confirmed by electrospray ionization mass spectrometry. The purities

Table 1 IC_{50} values for MC1 receptor and molecular weights (MW) of RGD-βAla-(Arg[11])CCMSH, RGD-Ahx-(Arg[11])CCMSH, RGD-Lys-(Arg[11])CCMSH, RGD-Arg-(Arg[11])CCMSH

Peptide	IC_{50} (nM)	Calculated MW (Da)	Measured MW (Da)
RGD-βAla-(Arg[11])CCMSH	0.8 ± 0.05	2,092.9	2,093.6
RGD-Ahx-(Arg[11])CCMSH	1.3 ± 0.1	2,136.4	2,136.1
RGD-Lys-(Arg[11])CCMSH[a]	2.1 ± 0.2	2,151.5	2,151.2
RGD-Arg-(Arg[11])CCMSH[a]	0.7 ± 0.05	2,177.9	2,178.2

[a] Data of RGD-Lys-(Arg[11])CCMSH, RGD-Arg-(Arg[11])CCMSH were cited from references (Yang et al. 2009, 2010b) for comparison

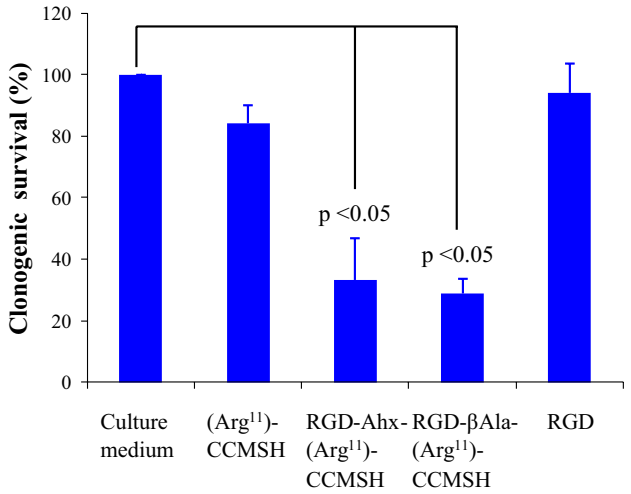

Fig. 2 Cytotoxic effects of RGD-βAla-(Arg[11])CCMSH and RGD-Ahx-(Arg[11])CCMSH in B16/F1 melanoma cells

of RGD-βAla-(Arg[11])CCMSH and RGD-Ahx-(Arg[11])CCMSH were 96.5 and 97.2 %, respectively. The molecular weights of RGD-βAla-(Arg[11])CCMSH and RGD-Ahx-(Arg[11])CCMSH are presented in Table 1. The measured molecular weights of RGD-βAla-(Arg[11])CCMSH and RGD-Ahx-(Arg[11])CCMSH were 2093.6 and 2136.1, respectively. The IC_{50} values of RGD-βAla-(Arg[11])CCMSH and RGD-Ahx-(Arg[11])CCMSH for MC1 receptor were 0.8 ± 0.05 and 1.3 ± 0.1 nM in B16/F1 melanoma cells (Table 1).

The cytotoxic effects of RGD-βAla-(Arg[11])CCMSH and RGD-Ahx-(Arg[11])CCMSH hybrid peptides were examined in B16/F1 melanoma cells. The results are presented in Fig. 2. The survival percentages of the peptide-treated groups were normalized taking the survival percentage of untreated group (in culture medium) as 100 %. Both RGD-βAla-(Arg[11])CCMSH and RGD-Ahx-(Arg[11])CCMSH exhibited remarkable cytotoxic effects in B16/F1 melanoma cells. The treatment of 0.1 μM of RGD-βAla-(Arg[11])CCMSH or RGD-Ahx-(Arg[11])CCMSH decreased the survival percentage by 71 and 67 %, respectively. In comparison with the untreated cells, the incubation with 0.1 μM of (Arg[11])CCMSH and RGD peptides decreased the survival percentage by 15 % ($p < 0.05$) and 6 % ($p > 0.05$), respectively.

The peptides were readily labeled with ^{99m}Tc with greater than 95 % radiolabeling yield. ^{99m}Tc-RGD-βAla-(Arg[11])CCMSH and ^{99m}Tc-RGD-Ahx-(Arg[11])CCMSH were completely separated from their excess non-labeled peptides by RP-HPLC. The retention times of ^{99m}Tc-RGD-βAla-(Arg[11])CCMSH and ^{99m}Tc-RGD-Ahx-(Arg[11])CCMSH were 12.3 and 16.2 min, whereas the retention times of RGD-βAla-(Arg[11])CCMSH and RGD-Ahx-(Arg[11])CCMSH were 10.6 and 11.4 min, respectively. Both ^{99m}Tc-RGD-βAla-(Arg[11])CCMSH and ^{99m}Tc-RGD-Ahx-(Arg[11])CCMSH were stable in mouse serum at 37 °C for 24 h. The melanoma targeting and pharmacokinetic properties of ^{99m}Tc-RGD-βAla-(Arg[11])CCMSH and ^{99m}Tc-RGD-Ahx-(Arg[11])CCMSH were determined in B16/F1 melanoma-bearing C57 mice. The biodistribution results of ^{99m}Tc-RGD-βAla-(Arg[11])CCMSH and ^{99m}Tc-RGD-Ahx-(Arg[11])CCMSH are shown in Tables 2 and 3. ^{99m}Tc-RGD-βAla-(Arg[11])CCMSH exhibited rapid and high tumor uptake in melanoma-bearing mice. The tumor uptake value was 14.37 ± 1.75 % ID/g at 0.5 h post-injection. The tumor uptake value of ^{99m}Tc-RGD-βAla-(Arg[11])CCMSH remained similar (14.67 ± 0.78 % ID/g) at 2 h post-injection. ^{99m}Tc-RGD-βAla-(Arg[11])CCMSH reached its peak tumor uptake value of 17.98 ± 2.49 % ID/g at 4 h post-injection. The tumor uptake value of ^{99m}Tc-RGD-βAla-(Arg[11])CCMSH gradually decreased to 8.63 ± 2.93 % ID/g at 24 h post-injection. Eighty-five percent of the tumor uptake of ^{99m}Tc-RGD-βAla-(Arg[11])CCMSH was blocked with 10 μg (6.1 nmol) of non-radiolabeled [Nle[4], D-Phe[7]]-α-MSH {NDP-MSH} at 2 h post-injection ($p < 0.05$), confirming that the tumor uptake was specific and MC1 receptor-mediated. Co-injection of ^{99m}Tc-RGD-βAla-(Arg[11])CCMSH with 3.5 μg (6.1 nmol) of RGD decreased 6 % of the tumor uptake ($p > 0.05$). Whole-body clearance of ^{99m}Tc-RGD-βAla-(Arg[11])CCMSH was rapid, with approximately 80 % of the injected radioactivity cleared through the urinary system by 2 h post-injection (Table 2). Normal organ uptake of ^{99m}Tc-RGD-βAla-(Arg[11])CCMSH was generally low (<1.7 % ID/g) except for the kidneys after 2 h post-injection. High tumor/blood and tumor/muscle uptake ratios were demonstrated as early as 2 h post-injection (Table 2). The renal uptake of ^{99m}Tc-RGD-βAla-(Arg[11])CCMSH reached its peak value of 25.64 ± 3.22 % ID/g at 0.5 h post-injection, and gradually decreased to 8.89 ± 0.84 % ID/g at 24 h post-injection.

^{99m}Tc-RGD-Ahx-(Arg[11])CCMSH exhibited similar biodistribution pattern as ^{99m}Tc-RGD-βAla-(Arg[11])CCMSH. Specifically, ^{99m}Tc-RGD-Ahx-(Arg[11])CCMSH displayed

Table 2 Biodistribution of ^{99m}Tc-RGD-βAla-(Arg^{11})CCMSH in B16/F1 melanoma-bearing C57 mice

Tissue	0.5 h	2 h	4 h	24 h	2 h NDP blockade	2 h RGD blockade
Percentage injected dose/gram (%ID/g)						
Tumor	14.37 ± 1.75	14.67 ± 0.78	17.98 ± 2.49	8.63 ± 2.93	2.14 ± 0.31*	13.80 ± 0.98
Brain	0.16 ± 0.02	0.06 ± 0.02	0.04 ± 0.02	0.03 ± 0.02	0.05 ± 0.01	0.02 ± 0.02
Blood	2.84 ± 0.40	0.43 ± 0.14	0.19 ± 0.04	0.06 ± 0.01	0.34 ± 0.01	0.02 ± 0.01
Heart	2.19 ± 0.48	0.63 ± 0.07	0.31 ± 0.10	0.29 ± 0.19	0.45 ± 0.22	0.65 ± 0.15
Lung	5.31 ± 0.55	1.20 ± 0.43	0.80 ± 0.20	0.37 ± 0.06	1.07 ± 0.40	1.26 ± 0.25
Liver	2.44 ± 0.17	1.54 ± 0.03	1.93 ± 0.35	1.21 ± 0.30	1.69 ± 0.23	1.40 ± 0.20
Skin	4.30 ± 0.53	1.14 ± 0.26	0.59 ± 0.29	0.59 ± 0.19	1.24 ± 0.09	1.02 ± 0.32
Spleen	2.07 ± 0.87	1.12 ± 0.08	0.83 ± 0.37	0.62 ± 0.48	0.72 ± 0.03	0.89 ± 0.38
Stomach	2.37 ± 0.43	1.68 ± 0.38	1.48 ± 0.50	0.82 ± 0.26	1.60 ± 0.27	1.59 ± 0.61
Kidneys	25.64 ± 3.22	16.31 ± 4.60	15.85 ± 3.55	8.89 ± 0.84	17.24 ± 1.35	17.22 ± 2.87
Muscle	0.87 ± 0.61	0.24 ± 0.12	0.15 ± 0.09	0.14 ± 0.06	0.29 ± 0.27	0.28 ± 0.09
Pancreas	0.90 ± 0.37	0.22 ± 0.07	0.23 ± 0.13	0.09 ± 0.04	0.26 ± 0.03	0.78 ± 0.64
Bone	1.52 ± 0.93	0.35 ± 0.25	0.49 ± 0.04	0.25 ± 0.16	0.57 ± 0.24	0.35 ± 0.35
Percentage injected dose (%ID)						
Intestines	3.47 ± 1.59	1.70 ± 0.16	2.11 ± 0.54	1.73 ± 0.18	2.25 ± 0.95	1.60 ± 0.64
Urine	51.28 ± 4.23	80.49 ± 2.43	82.32 ± 2.45	86.41 ± 2.14	82.37 ± 1.25	82.91 ± 5.27
Uptake ratio of tumor/normal tissue						
Tumor/blood	5.06	34.12	94.63	143.83	6.29	690.00
Tumor/kidneys	0.56	0.90	1.13	0.97	0.12	0.80
Tumor/lung	2.71	12.23	22.48	23.32	2.00	10.95
Tumor/liver	5.89	9.53	9.32	7.13	1.27	9.86
Tumor/muscle	16.52	61.13	119.87	61.64	7.38	49.29

The data was presented as percent injected dose/gram or as percent injected dose (mean ± SD, $n = 5$)

* $p < 0.05$, significance of differences in tumor and kidney uptake between ^{99m}Tc-RGD-βAla-(Arg^{11})CCMSH with or without peptide blockade at 2 h post-injection

similar renal uptake and lower tumor uptake at all time points investigated (Tables 2, 3). The tumor uptake value of ^{99m}Tc-RGD-Ahx-(Arg^{11})CCMSH was 9.92 ± 1.49 % ID/g at 0.5 h post-injection. ^{99m}Tc-RGD-Ahx-(Arg^{11})CCMSH reached its peak tumor uptake value of 11.85 ± 1.95 % ID/g at 2 h post-injection. The tumor uptake value of ^{99m}Tc-RGD-Ahx-(Arg^{11})CCMSH was 9.83 ± 1.03 % ID/g at 4 h post-injection, and gradually decreased to 5.51 ± 0.59 % ID/g at 24 h post-injection. Eighty-three percent of the tumor uptake of ^{99m}Tc-RGD-Ahx-(Arg^{11})CCMSH was blocked with 10 μg (6.1 nmol) of non-radiolabeled NDP-MSH at 2 h post-injection ($p < 0.05$), demonstrating that the tumor uptake was specific and MC1 receptor-mediated. Co-injection of ^{99m}Tc-RGD-Ahx-(Arg^{11})CCMSH with 3.5 μg (6.1 nmol) of RGD reduced 15 % of the tumor uptake ($p > 0.05$). Whole-body clearance of ^{99m}Tc-RGD-Ahx-(Arg^{11})CCMSH was rapid, with approximately 76 % of the injected radioactivity cleared through the urinary system by 2 h post-injection (Table 3). Normal organ uptake of ^{99m}Tc-RGD-Ahx-(Arg^{11})CCMSH was generally low (<2.2 % ID/g) except for the kidneys after 2 h post-injection. High tumor/blood and tumor/muscle uptake ratios were demonstrated as early as 2 h post-injection (Table 3). The renal uptake of ^{99m}Tc-RGD-Ahx-(Arg^{11})CCMSH reached its peak value of 24.03 ± 1.63 % ID/g at 0.5 h post-injection, and gradually decreased to 7.82 ± 1.66 % ID/g at 24 h post-injection.

The tumor to kidney uptake ratios of ^{99m}Tc-RGD-βAla-(Arg^{11})CCMSH and ^{99m}Tc-RGD-Ahx-(Arg^{11})CCMSH are summarized and compared with ^{99m}Tc-RGD-Lys-(Arg^{11})CCMSH and ^{99m}Tc-RGD-Arg-(Arg^{11})CCMSH in Fig. 3. ^{99m}Tc-RGD-Ahx-(Arg^{11})CCMSH showed higher tumor to kidney uptake ratios than ^{99m}Tc-RGD-Lys-(Arg^{11})CCMSH and ^{99m}Tc-RGD-Arg-(Arg^{11})CCMSH at 0.5, 2, 4, and 24 h post-injection. ^{99m}Tc-RGD-βAla-(Arg^{11})CCMSH exhibited the highest tumor to kidney uptake ratios among the ^{99m}Tc-labeled hybrid peptides at 0.5, 2, 4, and 24 h post-injection. Two B16/F1 melanoma-bearing C57 mice were injected with ^{99m}Tc-RGD-βAla-(Arg^{11})CCMSH or ^{99m}Tc-RGD-Ahx-(Arg^{11})CCMSH through the tail vein to visualize the tumors 2 h after dose administration. The representative whole-body SPECT/CT images

Table 3 Biodistribution of ^{99m}Tc-RGD-Ahx-(Arg^{11})CCMSH in B16/F1 melanoma-bearing C57 mice

Tissue	0.5 h	2 h	4 h	24 h	2 h NDP blockade	2 h RGD blockade
Percentage injected dose/gram (%ID/g)						
Tumor	9.92 ± 1.49	11.85 ± 1.95	9.83 ± 1.03	5.51 ± 0.59	1.97 ± 0.78*	10.08 ± 4.85
Brain	0.19 ± 0.05	0.06 ± 0.03	0.06 ± 0.03	0.02 ± 0.01	0.11 ± 0.03	0.06 ± 0.02
Blood	3.35 ± 0.10	0.70 ± 0.26	0.34 ± 0.11	0.05 ± 0.01	1.84 ± 0.24	0.02 ± 0.01
Heart	2.04 ± 0.42	0.75 ± 0.23	0.41 ± 0.16	0.16 ± 0.10	1.03 ± 0.14	0.32 ± 0.07
Lung	6.13 ± 0.43	1.78 ± 0.44	1.26 ± 0.53	0.54 ± 0.40	2.12 ± 0.76	1.53 ± 0.49
Liver	2.62 ± 0.22	1.72 ± 0.30	1.92 ± 0.3	0.78 ± 0.17	1.81 ± 0.17	1.39 ± 0.05
Skin	4.14 ± 0.84	1.08 ± 0.33	0.71 ± 0.36	0.28 ± 0.28	1.08 ± 0.94	1.16 ± 0.41
Spleen	2.12 ± 0.33	1.06 ± 0.59	1.29 ± 0.43	0.64 ± 0.35	1.69 ± 0.38	0.75 ± 0.45
Stomach	3.23 ± 0.69	2.18 ± 0.91	1.84 ± 0.84	0.35 ± 0.15	1.89 ± 0.04	1.70 ± 0.35
Kidneys	24.03 ± 1.63	16.88 ± 1.82	16.84 ± 1.75	7.82 ± 1.66	18.96 ± 2.89	17.98 ± 3.51
Muscle	0.74 ± 0.26	0.32 ± 0.11	0.3 ± 0.2	0.14 ± 0.17	0.33 ± 0.26	0.26 ± 0.10
Pancreas	0.93 ± 0.49	0.36 ± 0.08	0.14 ± 0.08	0.10 ± 0.03	0.44 ± 0.24	0.31 ± 0.06
Bone	1.69 ± 0.20	0.81 ± 0.20	0.33 ± 0.31	0.18 ± 0.15	0.74 ± 0.18	0.52 ± 0.06
Percentage injected dose (%ID)						
Intestines	3.54 ± 0.41	3.65 ± 1.83	3.99 ± 1.66	0.76 ± 0.36	3.73 ± 0.46	1.83 ± 0.17
Urine	47.11 ± 1.99	76.27 ± 5.99	80.65 ± 2.69	92.04 ± 1.76	77.84 ± 0.43	80.87 ± 1.8
Uptake ratio of tumor/normal tissue						
Tumor/blood	2.96	16.93	28.91	110.20	1.07	504.00
Tumor/kidneys	0.41	0.70	0.58	0.70	0.10	0.56
Tumor/lung	1.62	6.66	7.80	10.20	0.93	6.59
Tumor/liver	3.79	6.89	5.12	7.06	1.09	7.25
Tumor/muscle	13.41	37.03	32.77	39.36	5.97	38.77

The data was presented as percent injected dose/gram or as percent injected dose (mean ± SD, $n = 5$)

* $p < 0.05$, significance of differences in tumor and kidney uptake between ^{99m}Tc-RGD-Ahx-(Arg^{11})CCMSH with or without peptide blockade at 2 h post-injection

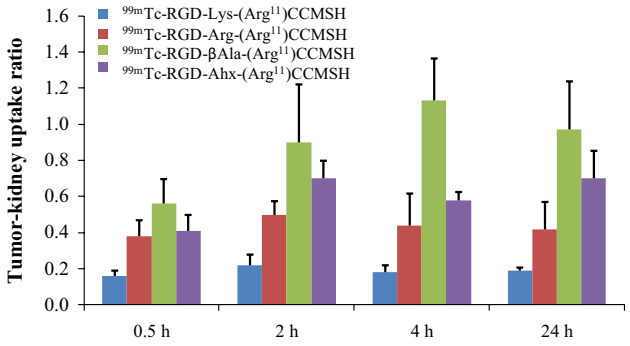

Fig. 3 Tumor to kidney uptake ratios of ^{99m}Tc-RGD-βAla-(Arg^{11})CCMSH, ^{99m}Tc-RGD-Ahx-(Arg^{11})CCMSH, ^{99m}Tc-RGD-Lys-(Arg^{11})CCMSH, and ^{99m}Tc-RGD-Arg-(Arg^{11})CCMSH at 0.5, 2, 4, and 24 h post-injection. The tumor to kidney uptake ratios of ^{99m}Tc-RGD-Lys-(Arg^{11})CCMSH and ^{99m}Tc-RGD-Arg-(Arg^{11})CCMSH were calculated based on the results published in the references (Yang et al. 2009, 2010b)

are presented in Fig. 4. Flank melanoma tumors were visualized clearly by both ^{99m}Tc-RGD-βAla-(Arg^{11})CCMSH or ^{99m}Tc-RGD-Ahx-(Arg^{11})CCMSH at 2 h post-injection. Both ^{99m}Tc-RGD-βAla-(Arg^{11})CCMSH or ^{99m}Tc-RGD-Ahx-(Arg^{11})CCMSH exhibited high tumor to normal organ uptake ratios except for the kidney. Compared to ^{99m}Tc-RGD-Ahx-(Arg^{11})CCMSH, ^{99m}Tc-RGD-βAla-(Arg^{11})CCMSH showed higher tumor to kidney imaging contrast.

The effects of L-lysine co-injection on the renal and tumor uptake of ^{99m}Tc-RGD-βAla-(Arg^{11})CCMSH and ^{99m}Tc-RGD-Ahx-(Arg^{11})CCMSH at 2 h post-injection are presented in Fig. 5 and compared with those of ^{99m}Tc-RGD-Lys-(Arg^{11})CCMSH and ^{99m}Tc-RGD-Arg-(Arg^{11})CCMSH. Co-injection of L-lysine did not affect the tumor uptake of all four ^{99m}Tc-RGD-X-(Arg^{11})CCMSH peptides. Co-injection of L-lysine significantly ($p < 0.05$) reduced the renal uptake of ^{99m}Tc-RGD-Lys-(Arg^{11})CCMSH from 67.12 ± 8.79 % ID/g to 32.20 ± 5.98 % ID/g, as well as significantly ($p < 0.05$) decreased the renal uptake of ^{99m}Tc-RGD-Arg-(Arg^{11})CCMSH from 43.01 ± 8.14 % ID/g to 31.10 ± 6.42 % ID/g. Interestingly, co-injection of L-lysine did not significantly decrease the renal uptake of ^{99m}Tc-RGD-βAla-(Arg^{11})CCMSH and ^{99m}Tc-RGD-Ahx-(Arg^{11})CCMSH.

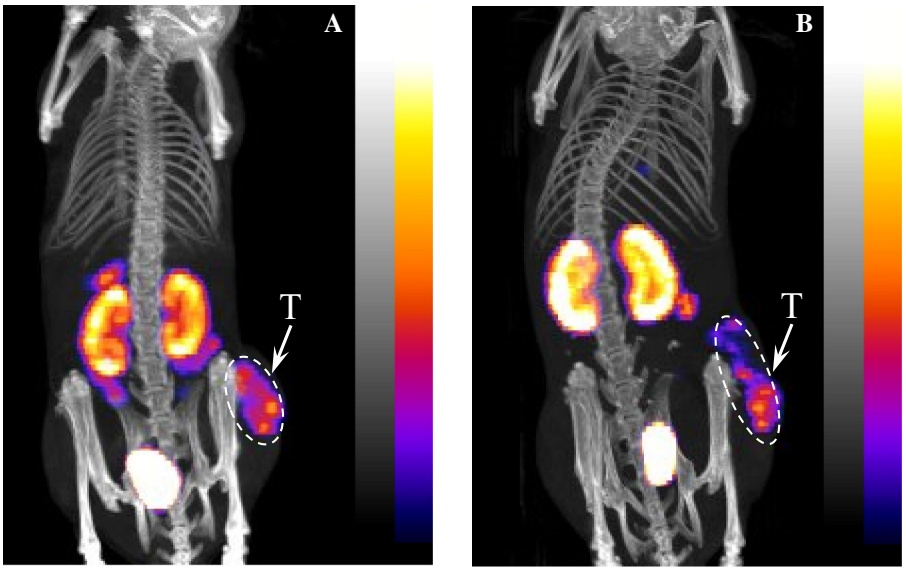

Fig. 4 Representative whole-body SPECT/CT images of ^{99m}Tc-RGD-βAla-(Arg^{11}) CCMSH (A) and ^{99m}Tc-RGD-Ahx-(Arg^{11})CCMSH (B) in B16/F1 melanoma-bearing C57 mice at 2 h post-injection. Tumor (T) lesions were highlighted with arrows on the images

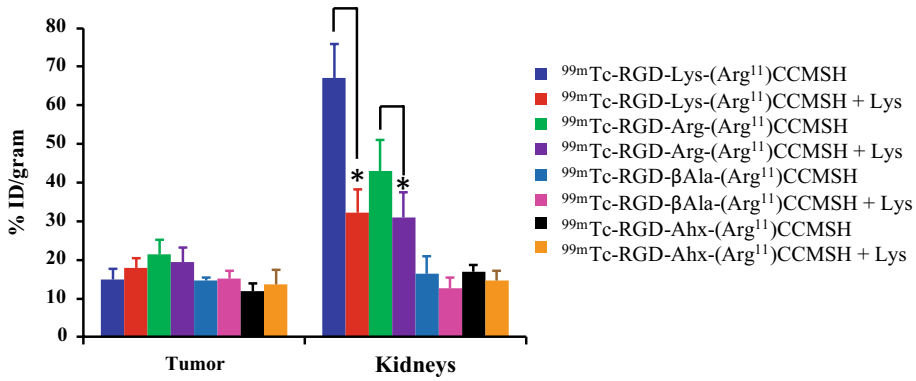

Fig. 5 Effect of L-lysine co-injection on the tumor and kidney uptake of ^{99m}Tc-RGD-X-(Arg^{11})CCMSH peptides (X = Lys, Arg, βAla, and Ahx) at 2 h post-injection. L-lysine co-injection significantly (*$p < 0.05$) reduced the renal uptake of ^{99m}Tc-RGD-Lys-(Arg^{11}) CCMSH by 52 % and the renal uptake of ^{99m}Tc-RGD-Arg-(Arg^{11}) CCMSH by 28 % without affecting their tumor uptake. On the other hand, L-lysine co-injection did not significantly reduce the renal uptake of ^{99m}Tc-RGD-βAla-(Arg^{11})CCMSH and ^{99m}Tc-RGD-Ahx-(Arg^{11})CCMSH. The results of ^{99m}Tc-RGD-Lys-(Arg^{11})CCMSH and ^{99m}Tc-RGD-Arg-(Arg^{11})CCMSH were cited from the references (Yang et al. 2009, 2010b)

Discussion

High mortality of malignant melanoma is associated with the occurrence of aggressive metastases. Novel and effective treatments are urgently needed to fulfill the desperate need for melanoma treatment since no curative treatment exists for metastatic melanoma. Recently, we have utilized the MC1 receptor-targeting (Arg^{11})CCMSH peptide as a delivery vehicle to transport the RGD motif into melanoma cells to induce apoptosis (Yang et al. 2009, 2010b). Both RGD-Lys-(Arg^{11})CCMSH and RGD-Arg-(Arg^{11}) CCMSH exhibited remarkable growth inhibition in B16/F1 melanoma cells. However, relatively high renal uptake of ^{99m}Tc-RGD-Lys-(Arg^{11})CCMSH and ^{99m}Tc-RGD-Arg-(Arg^{11})CCMSH needed to be decreased to facilitate their therapeutic applications. We demonstrated the contribution of the overall positive charges of ^{99m}Tc-RGD-Lys-(Arg^{11}) CCMSH and ^{99m}Tc-RGD-Arg-(Arg^{11})CCMSH to their non-specific renal uptake through L-lysine co-injection in our previous work (Yang et al. 2009, 2010b). Hence, we designed two new α-MSH hybrid peptides with less overall positive charges to examine whether the reduction of the overall positive charge of the ^{99m}Tc-labeled α-MSH hybrid peptides could further reduce their renal uptake in this study. Specifically, we substituted the positively-charged Lys or Arg linker with the neutral βAla or Ahx linker to generate RGD-βAla-(Arg^{11})CCMSH and RGD-Ahx-(Arg^{11})CCMSH.

The replacement of the positively-charged Lys or Arg linker with the neutral βAla or Ahx linker did maintain the

low nanomolar MC1 receptor-binding affinities of RGD-βAla-(Arg^{11})CCMSH and RGD-Ahx-(Arg^{11})CCMSH. RGD-βAla-(Arg^{11})CCMSH displayed comparable IC_{50} value as RGD-Arg-(Arg^{11})CCMSH (0.8 vs. 0.7 nM), whereas RGD-Ahx-(Arg^{11})CCMSH showed similar IC_{50} value as RGD-Lys-(Arg^{11})CCMSH (1.3 vs. 2.1 nM). The difference in receptor-binding affinity between the RGD-βAla-(Arg^{11})CCMSH and RGD-Ahx-(Arg^{11})CCMSH was attributed to the length of the hydrocarbon between the βAla linker and Ahx linker. The βAla linker has 2 hydrocarbons, whereas the Ahx linker has 5 hydrocarbons. The IC_{50} value of RGD-βAla-(Arg^{11})CCMSH was lower than that of RGD-Ahx-(Arg^{11})CCMSH, indicating that the shorter hydrocarbon linker makes the RGD-βAla-(Arg^{11})CCMSH peptide better fit in the receptor-binding pocket for enhanced receptor-binding affinity in vitro. The length of the hydrocarbon linker also displayed a profound impact on the receptor-binding affinities of DOTA-conjugated bombesin peptides (Garrison et al. 2008; Hoffman et al. 2003). The hydrocarbon linkers ranging from 5-carbon to 8-carbon between the DOTA and bombesin peptide resulted in 0.6–1.7 nM receptor-binding affinities for bombesin peptides (Garrison et al. 2008). Either shorter or longer hydrocarbon linkers dramatically reduce the receptor-binding affinity by 100-fold. The difference in linker length between the α-MSH and bombesin peptides demonstrated that it is necessary to carefully investigate which linker is suitable for optimal tumor uptake when switching from one type of peptide to another type of peptide.

It is worthwhile to note that the (Arg^{11})CCMSH moiety serves as a site-specific chelating system for direct labeling of ^{99m}Tc. Specifically, three –SH groups from Cys^3, Cys^4, and Cys^{10} and one –NH group from Cys^4 form a NS_3 chelating system for ^{99m}Tc. ^{99m}Tc-RGD-Arg-(Arg^{11})CCMSH exhibited more favorable pharmacokinetic properties than ^{99m}Tc-RGD-Lys-(Arg^{11})CCMSH in our previous report (Yang et al. 2009, 2010b). Specifically, ^{99m}Tc-RGD-Arg-(Arg^{11})CCMSH displayed 44 % higher tumor uptake and 33 % less renal uptake than ^{99m}Tc-RGD-Lys-(Arg^{11})CCMSH at 2 h post-injection (Yang et al. 2009, 2010b). In this study, the replacement of the positively-charged Lys or Arg linker with the neutral βAla or Ahx linker dramatically decreased the renal uptake values of ^{99m}Tc-labeled RGD-βAla-(Arg^{11})CCMSH and RGD-Ahx-(Arg^{11})CCMSH in B16/F1 melanoma-bearing C57 mice. Compared to ^{99m}Tc-RGD-Arg-(Arg^{11})CCMSH, both ^{99m}Tc-RGD-βAla-(Arg^{11})CCMSH and ^{99m}Tc-RGD-Ahx-(Arg^{11})CCMSH exhibited very similar lower renal uptake values at all time points investigated. The renal uptake values of ^{99m}Tc-RGD-βAla-(Arg^{11})CCMSH were 69, 38, 43, and 55 % of ^{99m}Tc-RGD-Arg-(Arg^{11})CCMSH at 0.5, 2, 4, and 24 h post-injection, respectively. As we anticipated, ^{99m}Tc-RGD-βAla-(Arg^{11})CCMSH displayed higher tumor uptake than ^{99m}Tc-RGD-Ahx-(Arg^{11})CCMSH. The tumor uptake of ^{99m}Tc-RGD-βAla-(Arg^{11})CCMSH were 1.4, 1.2, 1.8, and 1.6 times the tumor uptake of ^{99m}Tc-RGD-Ahx-(Arg^{11})CCMSH at 0.5, 2, 4 and 24 h post-injection, respectively. Dramatic decrease in the renal uptake of ^{99m}Tc-RGD-βAla-(Arg^{11})CCMSH and ^{99m}Tc-RGD-Ahx-(Arg^{11})CCMSH enhanced the tumor to kidney uptake ratios. The tumor to kidney uptake ratio of ^{99m}Tc-RGD-Ahx-(Arg^{11})CCMSH was 1.1, 1.4, 1.2, and 1.8 times the tumor to kidney uptake ratio of ^{99m}Tc-RGD-Arg-(Arg^{11})CCMSH at 0.5, 2, 4, and 24 h post-injection, respectively. Among these four ^{99m}Tc-labeled RGD-conjugated α-MSH hybrid peptides (Fig. 3), ^{99m}Tc-RGD-βAla-(Arg^{11})CCMSH exhibited the highest tumor to kidney uptake ratios. The tumor to kidney uptake ratio of ^{99m}Tc-RGD-βAla-(Arg^{11})CCMSH was 1.5, 1.9, 2.4, and 2.3 times the tumor to kidney uptake ratio of ^{99m}Tc-RGD-Arg-(Arg^{11})CCMSH at 0.5, 2, 4, and 24 h post-injection, respectively. The SPECT/CT images of ^{99m}Tc-RGD-βAla-(Arg^{11})CCMSH and ^{99m}Tc-RGD-Ahx-(Arg^{11})CCMSH (Fig. 4) also confirmed better tumor to kidney imaging contrast for ^{99m}Tc-RGD-βAla-(Arg^{11})CCMSH than that for ^{99m}Tc-RGD-Ahx-(Arg^{11})CCMSH.

Non-specific renal uptake of peptides is mainly caused by glomerular filtration and tubular reabsorption (Maack et al. 1979; Mørgenson et al. 1977; Silbernagl et al. 1988) because peptides are generally filtered in the glomerulus and reabsorbed in the cells of the proximal tubule. Positively-charged peptides can bind to the negatively-charged tubule cells through electrostatic interaction. Thus, positively-charged amino acids such as L-lysine and L-arginine could be used to decrease the renal uptake of radiolabeled peptides by shielding such electrostatic interaction (Béhé et al. 2005; Behr et al. 1995, 1996). Over the past several years, both colchicine and megalin were reported to be involved in the renal uptake of ^{111}In-DTPA-Octreotide (Christensen et al. 1998; De Jong et al. 2005; Rolleman et al. 2004). The use of colchicine prevented endocytosis in tubular cells, thus decreased the renal uptake up to 25 % in a rat model (Rolleman et al. 2004). Recently, more research efforts have focused on decreasing the renal reabsorption of radiolabeled peptides through interfering with endocytic receptors on the proximal tubular cells. Specifically, megalin is a multiligand receptor which has four cysteine-rich ligand-binding domains. Thus, various structurally different peptides and proteins (i.e., albumin and vitamin D-binding protein) can bind to megalin. For instance, albumin-derived peptides efficiently decreased the renal uptake of radiolabeled peptides by 26–88 % (Vegt et al. 2012). Although the mechanism has not been completely identified, interestingly, it was reported that charges may play an important role in megalin-ligand binding (Birn et al. 2006; Gotthardt et al. 2007; Orlando et al. 1997). In this study, we managed to reduce the renal uptake through structural

modification of the peptides. The substitution of the positively-charged Lys or Arg linker with the neutral βAla or Ahx linker dramatically decreased the non-specific renal uptake of ^{99m}Tc-RGD-βAla-(Arg^{11})CCMSH and ^{99m}Tc-RGD-Ahx-(Arg^{11})CCMSH. Moreover, co-injection of L-lysine significantly ($p < 0.05$) reduced the renal uptake of ^{99m}Tc-RGD-Lys-(Arg^{11})CCMSH and ^{99m}Tc-RGD-Arg-(Arg^{11})CCMSH by 52 and 28 % at 2 h post-injection, respectively. These results suggested that the switch from the positively-charged Lys and Arg to neutral βAla and Ahx linkers substantially reduced the electrostatic interactions between the peptides and tubule cells in kidneys. Interestingly, co-injection of L-lysine did not significantly decrease the renal uptake of ^{99m}Tc-RGD-βAla-(Arg^{11})CCMSH and ^{99m}Tc-RGD-Ahx-(Arg^{11})CCMSH. Further studies need to be performed to understand whether the renal uptake of ^{99m}Tc-RGD-βAla-(Arg^{11})CCMSH and ^{99m}Tc-RGD-Ahx-(Arg^{11})CCMSH is related to the endocytic receptors on the proximal tubular cells.

Both RGD-βAla-(Arg^{11})CCMSH and RGD-Ahx-(Arg^{11})CCMSH exhibited remarkable cytotoxicity in B16/F1 melanoma cells. Single treatment with 0.1 μM of RGD-βAla-(Arg^{11})CCMSH or RGD-Ahx-(Arg^{11})CCMSH decreased the survival percentage by 71 and 67 %, respectively. The treatment with 0.1 μM of RGD peptide did not reduce the survival percentage of B16/F1 cells significantly ($p > 0.05$), indicating that the internalization of RGD-βAla-(Arg^{11})CCMSH and RGD-Ahx-(Arg^{11})CCMSH played a key role in their cytotoxicity. Although the treatment of 0.1 μM of (Arg^{11})CCMSH peptide reduced the survival percentage of B16/F1 cells by 15 % ($p < 0.05$), the reduction in survival percentage of RGD-βAla-(Arg^{11})CCMSH and RGD-Ahx-(Arg^{11})CCMSH was 4.8 and 4.5 times the reduction in survival percentage of (Arg^{11})CCMSH. Dramatic difference in cytotoxicity between RGD-βAla-(Arg^{11})CCMSH/RGD-Ahx-(Arg^{11})CCMSH and (Arg^{11})CCMSH demonstrated that the cytotoxic effects of RGD-βAla-(Arg^{11})CCMSH and RGD-Ahx-(Arg^{11})CCMSH hybrid peptides were due to the apoptotic effect of the RGD motif in the hybrid peptide. The cytotoxic effects generated by the treatments of RGD-βAla-(Arg^{11})CCMSH and RGD-Ahx-(Arg^{11})CCMSH highlighted the potential of treating the melanoma with the targeted radiation and apoptosis inducer. High-energy beta-emitter ^{188}Re is a therapeutic radionuclide and shares similar coordination chemistry with ^{99m}Tc. Thus, the RGD-conjugated hybrid peptide could be directly labeled with ^{188}Re for melanoma treatment without peptide structural modification. ^{99m}Tc-RGD-βAla-(Arg^{11})CCMSH showed more favorable pharmacokinetic properties than ^{99m}Tc-RGD-Ahx-(Arg^{11})CCMSH in this study. The enhanced tumor to kidney uptake ratio of ^{99m}Tc-RGD-βAla-(Arg^{11})CCMSH would facilitate the potential application of ^{188}Re-RGD-βAla-(Arg^{11})CCMSH for melanoma treatment in the future.

Conclusions

The replacement of the positively-charged Arg linker with the neutral βAla or Ahx linker dramatically decreased the non-specific renal uptake of ^{99m}Tc-RGD-βAla-(Arg^{11})CCMSH and ^{99m}Tc-RGD-Ahx-(Arg^{11})CCMSH by 62 and 61 % at 2 h post-injection. ^{99m}Tc-RGD-βAla-(Arg^{11})CCMSH displayed higher melanoma uptake than ^{99m}Tc-RGD-Ahx-(Arg^{11})CCMSH at 0.5, 2, 4, and 24 h post-injection. Dramatically enhanced tumor to kidney ratio of ^{99m}Tc-RGD-βAla-(Arg^{11})CCMSH warranted the evaluation of ^{188}Re-RGD-βAla-(Arg^{11})CCMSH as a novel MC1 receptor-targeting therapeutic peptide for melanoma treatment in the future.

Acknowledgments We appreciate Dr. Fabio Gallazzi for his technical assistance. This work was supported by the NIH grant NM-INBRE P20RR016480/P20GM103451. The SPECT/CT images in this article were generated by the Keck-UNM Small Animal Imaging Resource established with funding from the W.M. Keck Foundation and the University of New Mexico Cancer Research and Treatment Center (NIH P30 CA118100).

Conflict of interest The authors declare that they have no conflict of interest.

References

Béhé M, Kluge G, Becker W, Gotthardt M, Behr TM (2005) Use of polyglutamic acids to reduce uptake of radiometal-labeled minigastrin in the kidneys. J Nucl Med 46:1012–1015

Behr TM, Sharkey RM, Juweid ME, Blumenthal RD, Dunn RM, Bair HJ, Wolf FG, Becker WS, Goldenberg DM (1995) Reduction of the renal uptake of radiolabeled monoclonal antibody fragments by cationic amino acids and their derivatives. Cancer Res 55:3825–3834

Behr TM, Becker WS, Sharkey RM, Juweid ME, Dunn RM, Bair HJ, Wolf FG, Goldenberg DM (1996) Reduction of renal uptake of monoclonal antibody fragments by amino acid infusion. J Nucl Med 37:829–833

Birn H, Christensen EI (2006) Renal albumin absorption in physiology and pathology. Kidney Int 69:440–449

Chen J, Cheng Z, Hoffman TJ, Jurisson SS, Quinn TP (2000) Melanoma-targeting properties of ^{99m}technetium-labeled cyclic alpha-melanocyte-stimulating hormone peptide analogues. Cancer Res 60:5649–5658

Chen J, Cheng Z, Owen NK, Hoffman TJ, Miao Y, Jurisson SS, Quinn TP (2001) Evaluation of an ^{111}In-DOTA-rhenium cyclized α-MSH analog: a novel cyclic-peptide analog with improved tumor-targeting properties. J Nucl Med 42:1847–1855

Cheng Z, Chen J, Miao Y, Owen NK, Quinn TP, Jurisson SS (2002) Modification of the structure of a metallopeptide: synthesis and biological evaluation of ^{111}In-labeled DOTA-conjugated rhenium-cyclized alpha-MSH analogues. J Med Chem 45:3048–3056

Cheng Z, Xiong Z, Subbarayan M, Chen X, Gambhir SS (2007) ^{64}Cu-labeled alpha-melanocyte-stimulating hormone analog for MicroPET imaging of melanocortin 1 receptor expression. Bioconjug Chem 18:765–772

Christensen EI, Birn H, Verroust P, Moestrup SK (1998) Megalin-mediated endocytosis in renal proximal tubule. Ren Fail 20:191–199

De Jong M, Barone R, Krenning EP, Bernard BF, Melis M, Vissor T, Gekle M, Willnow TE, Walrand S, Jamar F, Pauwels S (2005) Megalin is essential for renal proximal tubule reabsorption of ^{111}In-DTPA-Octreotide. J Nucl Med 46:1696–1700

Froidevaux S, Calame-Christe M, Tanner H, Sumanovski L, Eberle AN (2002) A novel DOTA-alpha-melanocyte-stimulating hormone analog for metastatic melanoma diagnosis. J Nucl Med 43:1699–1706

Froidevaux S, Calame-Christe M, Schuhmacher J, Tanner H, Saffrich R, Henze M, Eberle AN (2004) A gallium-labeled DOTA-alpha-melanocyte-stimulating hormone analog for PET imaging of melanoma metastases. J Nucl Med 45:116–123

Froidevaux S, Calame-Christe M, Tanner H, Eberle AN (2005) Melanoma targeting with DOTA-alpha-melanocyte-stimulating hormone analogs: structural parameters affecting tumor uptake and kidney uptake. J Nucl Med 46:887–895

Garrison JC, Rold TL, Sieckman GL, Naz F, Sublett SV, Figueroa SD, Volkert WA, Hoffman TJ (2008) Evaluation of the pharmacokinetic effects of various linking group using the ^{111}In-DOTA-X-BBN(7-14)NH_2 structural paradigm in a prostate cancer model. Bioconjug Chem 19:1803–1812

Gotthardt M, van Eerd-Vismale J, Oyen WJ, De Jong M, Zhang H, Rolleman E, Maecke HR, Béhé M, Boerman OC (2007) Indication for different mechanisms of kidney uptake of radiolabeled peptides. J Nucl Med 48:596–601

Guo H, Shenoy N, Gershman BM, Yang J, Sklar LA, Miao Y (2009a) Metastatic melanoma imaging with an ^{111}In-labeled lactam bridge-cyclized alpha-melanocyte-stimulating hormone peptide. Nucl Med Biol 36:267–276

Guo H, Yang J, Gallazzi F, Prossnitz ER, Sklar LA, Miao Y (2009b) Effect of DOTA position on melanoma targeting and pharmacokinetic properties of ^{111}In-labeled lactam bridge-cyclized α-melanocyte stimulating hormone peptide. Bioconjug Chem 20:2162–2168

Guo H, Yang J, Shenoy N, Miao Y (2009c) Gallium-67-labeled lactam bridge-cyclized alpha-melanocyte stimulating hormone peptide for primary and metastatic melanoma imaging. Bioconjug Chem 20:2356–2363

Guo H, Yang J, Gallazzi F, Miao Y (2010) Reduction of the ring size of radiolabeled lactam bridge-cyclized alpha-MSH peptide resulting in enhanced melanoma uptake. J Nucl Med 51:418–426

Hoffman TJ, Gali H, Smith CJ, Sieckman GL, Hayes DL, Owen NK, Volkert WA (2003) Novel series of ^{111}In-labeled bombesin analogs as potential radiopharmaceuticals for specific targeting of gastrin-releasing peptide receptors expressed on human prostate cancer cells. J Nucl Med 44:823–831

Maack T, Johnson V, Kan ST, Figueiredo J, Sigulem D (1979) Renal filtration, transport, and metabolism of low molecular weight proteins: a review. Kidney Int 16:251–270

Miao Y, Owen NK, Whitener D, Gallazzi F, Hoffman TJ, Quinn TP (2002) In vivo evaluation of ^{188}Re-labeled alpha-melanocyte stimulating hormone peptide analogs for melanoma therapy. Int J Cancer 101:480–487

Miao Y, Whitener D, Feng W, Owen NK, Chen J, Quinn TP (2003) Evaluation of the human melanoma targeting properties of radiolabeled alpha-melanocyte stimulating hormone peptide analogues. Bioconjug Chem 14:1177–1184

Miao Y, Owen NK, Fisher DR, Hoffman TJ, Quinn TP (2005a) Therapeutic efficacy of a ^{188}Re-labeled alpha-melanocyte-stimulating hormone peptide analog in murine and human melanoma-bearing mouse models. J Nucl Med 46:121–129

Miao Y, Hylarides M, Fisher DR, Shelton T, Moore H, Wester DW, Fritzberg AR, Winkelmann CT, Hoffman TJ, Quinn TP (2005b) Melanoma therapy via peptide-targeted alpha-radiation. Clin Cancer Res 11:5616–5621

Miao Y, Benwell K, Quinn TP (2007) ^{99m}Tc- and ^{111}In-labeled alpha-melanocyte-stimulating hormone peptides as imaging probes for primary and pulmonary metastatic melanoma detection. J Nucl Med 48:73–80

Miao Y, Gallazzi F, Guo H, Quinn TP (2008) ^{111}In-labeled lactam bridge-cyclized alpha-melanocyte stimulating hormone peptide analogues for melanoma imaging. Bioconjug Chem 19:539–547

Mørgenson CE, Sølling K (1977) Studies on renal tubular protein reabsorption: partial and near complete inhibition by certain amino acids. Scand J Clin Lab Invest 37:477–486

Orlando RA, Exner M, Czekay RP, Yamazaki H, Saito A, Ullrich R, Kerjaschki D, Farquhar MG (1997) Identification of the second cluster of ligand-binding repeats in megalin as a site for receptor-ligand interactions. Proc Natl Acad Sci USA 94:2368–2373

Rolleman EJ, Krenning EP, Van Gameren A, Bernard BF, De Jong M (2004) Uptake of [^{111}In-DTPA0]octreotide in the rat kidney is inhibited by colchicine and not by fructose. J Nucl Med 45:709–713

Siegrist W, Solca F, Stutz S, Giuffre L, Carrel S, Girard J, Eberle AN (1989) Characterization of receptors for alpha-melanocyte-stimulating hormone on human melanoma cells. Cancer Res 49:6352–6358

Silbernagl S (1988) The renal handling of amino acids and oligopeptides. Physio Rev 68:912–986

Tatro JB, Reichlin S (1987) Specific receptors for alpha-melanocyte-stimulating hormone are widely distributed in tissues of rodents. Endocrinology 121:1900–1907

Vegt E, Eek A, Oyen WJG, De Jong M, Gotthardt M, Boerman OC (2012) Albumin-derived peptides efficiently reduce renal uptake of radiolabelled peptides. Eur J Nucl Med Mol Imaging 37:226–234

Wei L, Butcher C, Miao Y, Gallazzi F, Quinn TP, Welch MJ, Lewis JS (2007) Synthesis and biologic evaluation of ^{64}Cu-labeled rhenium-cyclized alpha-MSH peptide analog using a cross-bridged cyclam chelator. J Nucl Med 48:64–72

Yang J, Guo H, Gallazzi F, Berwick M, Padilla RS, Miao Y (2009) Evaluation of a novel RGD-conjugated alpha-melanocyte stimulating hormone hybrid peptide for potential melanoma therapy. Bioconjug Chem 20:1634–1642

Yang J, Guo H, Miao Y (2010a) Technetium-99m-labeled Arg-Gly-Asp-conjugated alpha-melanocyte stimulating hormone hybrid peptides for human melanoma imaging. Nucl Med Biol 37:873–883

Yang J, Guo H, Padilla RS, Berwick M, Miao Y (2010b) Replacement of the Lys linker with an Arg linker resulting in improved melanoma uptake and reduced renal uptake of Tc-99m-labeled Arg-Gly-Asp-conjugated alpha-melanocyte stimulating hormone hybrid peptide. Bioorg Med Chem 18:6695–6700